PHOTOVOLTAIC AND CHARGE CARRIER TRANSPORT PARAMETERS OF PTOPT

By
Bizuneh G/michael

A THESIS PRESENTED TO
THE SCHOOL OF GRADUATE STUDIES
ADDIS ABABA UNIVERSITY
IN PARTIAL FULFILLMENT OF THE REQUIREMENTS
FOR THE DEGREE OF

MASTER OF SCIENCE in PHYSICS

ADDIS ABABA, ETHIOPIA
AUGUST 2007

ADDIS ABABA UNIVERSITY

DEAPRMENT OF PHYSICS

The undersigned hereby certify that they have read and recommend to the Faculty of Science for acceptance of an MSc Thesis entitled "**Photovoltaic and Charge Carrier Transport parameters of PTOPT**" by **Bizuneh G/michael Master of Science**.

Dated: August 2007

Supervisor: _____

Dr. Genene Tessema

Examiners: _____

Dr. Mulugeta Bekele

_____

Prof. Singh P.

This Work is Dedicated to My Parents

Table of Contents

List of Tables

List of Figures

List of Figures

List of Tables

Acknowledgements

I am very grateful for my advisor Dr. Genene Tessema, best Ethiopian Physicist, for introducing me with this field of study and his urge throughout this work. The ministry of Education for the sponsorship of this MSc Program. Engineer Ehite Gebremichael, who never get tired to provide me the right thing that I need to have, you are a perfect women, God bless you. My precious Emaye and Abaye, I love you very much. Kuri(with her family), koki, and Wole you are simply the ultimate source of today's me. Yoni, Eli and Yiete you are my hero brothers, thank you for all your good thoughts to me. Kidus Gashaw, I will never forget you for your delicious friendship.

Addis Ababa University

March, 2007

Abstract

Low cost and easy processability of organic electronic and photonic devices, which is made from conductive polymer make them to be called a 'noble materials'. The rise of the idea of "self healing" materials, especially polymeric materials[21], seems to make a remarkable change on the short lifetime of the device which is made of organic polymers. As a consequence, a rapid and definite analysis of different physical phenomenons in polymeric devices is expected from the theoretical as well as the the experimental physics. In this thesis, the photovoltaic and charge transport properties of the photovoltaic cells made from poly[3-(4-octylphenyl)-2,2'-bithiophene](PTOPT) was studied. A Schottky diode is prepared from a single layer polymer sandwiched in Al and PEDOT:PSS/ITO electrode. That is **Al/PTOPT/PEDOT:PSS/ITO** layered device structure. By applying a forward bias voltage, the current value for different voltage is measured and found that a rectifying contact is formed. Then, under AM 1.5 (one sun) illumination, the J-V data was collected and a power conversion efficiency of 0.35% is recorded. Furthermore, dark current-voltage measurement is made by reversing the polarity of the electrodes. The symmetric nature of the J-V semi-logarithmic plot reveals that there is a unipolar charge injection in both sides of the electrodes. As the consequence, from the space charge limited region of the J-V data, we studied the electric field dependence of the hole transport in the device and we determined the zero field mobility ($\mu_o = (2.25 \pm 0.12) \times 10^{-10} m^2/Vs$) and the field activation factor ($\gamma = (7.01 \pm 0.58) \times 10^{-5} (m/V)^{\frac{1}{2}}$).

Chapter 1

Introduction

Polymers are macromolecules made from several repeating units called monomers. The repeating units are linked by covalent bonds. Their chemical skeletal structures can be linear, cyclic or branched. A polymer consisting of only one type of repeating unit is called a homopolymer. On the other hand, a polymer consisting of two or more repeating units is called a copolymer or a heteropolymer. Some examples of natural polymers are rubber, starch, cellulose, DNA and collagen.

Conjugated polymers, which have alternative single and double carbon bonds in their back bone, have attracted considerable interest since the first conjugated-polymer-based light emitting diodes (LEDs) were created in 1990. Polymers belonging to the conjugated polymer family are capable of acting as conducting or semiconducting materials and are used in polymer-based optoelectronics devices, such as light emitting diodes, photovoltaic solar cells, and field effect transistors. These devices usually contain several conjugated polymer layers that are prepared from an organic solution of the polymers. The fascinating process of photosynthesis in green plants and the retinal molecule, which is covalently attached to the protein rhodopsin in the retina of the eye, are examples of how nature makes use of conjugated molecules.

As the global energy demand continues to increase every year, the limiting supply of todays main energy sources (i.e. oil, coal, uranium) and their detrimental long-term effects on the natural balance on our planet, underscore the urgency of developing renewable energy sources which neither run out nor have any significant harmful

effects on the environment. Harvesting energy directly from the sun using photovoltaic (PV) technology is being widely recognized as an essential component of future global energy production. Conventional photovoltaic devices (PVDs) are fabricated from inorganic semiconductor materials such as crystalline silicon (Si) and they are already available on the market. Fabrication of inorganic semiconductor based solar cells demands expensive technologies for purification, patterning and various coating processes. However, if photovoltaic devices are to be considered as the major future global energy sources, large-scale manufacturing at reasonably low cost is desired. The cost reduction can be realized by using semiconducting materials that can be processed using few steps and cheap technologies. Thus, there has been considerable effort in developing thin film technologies that enable significant cost reductions. In the last few years, solar cells based on thin and multijunction inorganic films have emerged as alternatives to crystalline Si based solar cells. These solar cells are fabricated by using cheap techniques such as sputtering and physical vapor deposition. Currently, they are relatively cheaper but less efficient as compared to Si based solar cells. In general, achieving competitive, cost effective and efficient PVDs may require new materials, concepts and technologies.

The field of conjugated polymer-based electronics is rapidly expanding in areas wherever low cost, flexibility and lightweight is desirable. Currently, conjugated polymers have become candidates for several applications such as PVDs integrated electronic circuits based on field effect transistors and flat displays based on light emitting diodes.

Among the many PVD architecture a single layer structure is the simplest one to study different properties of the semiconductor (an active layer for converting the visible part of the electromagnetic wave to electron-hole pair), that we use. A single layer PSCs rely on a semiconducting polymer which is usually sandwiched between two asymmetric work function metals acting as anode and cathode. In such films, photo generated electron-hole pairs (excitons) are separated at a rectifying interface (Schottky contact) the free carriers are then collected by the respective electrodes. The polymer films are processed from solutions mainly through spin coating method, which is quite easy and cheap for experimental purpose. The top electrode (cathode), in our laboratory, is constructed through thermal evaporation techniques while the bottom electrode

(anode) is constructed from a glass substrate coated with thin conducting films.
In this thesis several issues concerning the photovoltaic parameters of solar cells with a single layer polymer films are addressed. We studied a thiophene derivative polymer, poly[3-(4-octylphenyl)-2,2'-bithiophene](PTOPT). We used a sandwich structure of **Al/PTOPT/PEDOT:PSS/ITO** on a glass substrate. PEDOT:PSS is a transparent polymer, it has become a universal hole conducting layer in polymer based solar cells and light emitting diodes. Using the current-voltage measurement we characterize the photovoltaic properties and parameters of this sandwich structure.
One of the main parameters limiting the efficiency of a polymer solar cell is the charge carrier transport properties in the active layer of the polymer diode. The transport parameters and their relation to the inherent material parameters are addressed based on experimental data and theoretical models of charge transport in disordered medias. The effect of charge transport on efficiency of solar cells is quite tremendous. In particular, as far as PSCs are concerned, the low hole mobility in most conjugated polymers contributes a lot towards reduction of power conversion efficiency. In this thesis we try to investigate some of the charge carrier transport properties and parameters in PTOPT.
In chapter two, different properties of polymer, for instance its conductivity and solubility will be reviewed. After that we will see what photovoltaic effect is, how photovoltaic device will be constructed and how to characterize our photovoltaic device. Chapter four of this thesis is about charge carriers transport in disordered materials. Since there is energetic and spatial disorder in polymer films, there is no definite transport of charge carriers. However, the Poole-Frankel empirical mobility equation, which deals on electric field dependance of the mobility of charge carriers and the space charge limited region of the I-V characteristics helps us to study charge carrier transport in the active region of solar cell device (PTOPT). In chapter five we will see how we prepare our samples and data measurement. Finally chapter six will discuss the results that we obtain in our experimental study.

Chapter 2

General Properties of Polymer for Solar Cell

2.1 Structural Properties of Organic Semiconductors

Every conjugated polymer has a unique chemical structure that determines its optical and electrical behavior. Figure 2.1 is the chemical structure of the polymer that we used in our study. Each chain of a conjugated polymer does not stretch indefinitely but rather makes twists and coiled structures resulting into the amorphous nature of a polymer. This disordered morphology limits the delocalization length of the π electron cloud to a definite length known as a conjugation length. This characteristic length is bounded by an energy barrier, which may be created by defects or kinks. On the other hand, the conjugation length segments have random distributions leading to different energies of the π electrons. This is clearly manifested in the featureless, broad absorption and emission spectra of conjugated polymers.

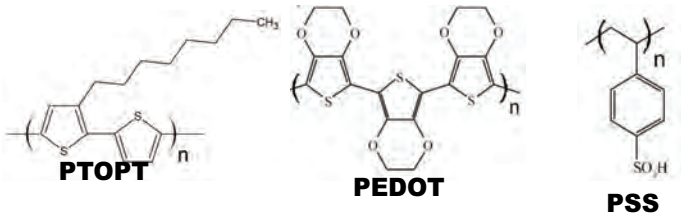

Figure 2.1: The chemical structures of the polymers that we use in our study

2.2 The origin of semiconducting behavior

The fundamental source of semiconducting property of conjugated polymers originates from the overlap of the molecular orbitals formed by the valence electrons of chemically bonded C-atoms. A neutral carbon atom has six electrons, which occupy the 1s, 2s and 2p orbitals giving a ground state electronic configuration of $(1s^2, 2s^2, 2p^2)$. The atomic orbitals of carbon are modified into hybrid orbitals as they form covalent bonds. When a carbon atom forms a bond with another carbon atom, a 2s-electron is promoted to the vacant 2p-orbital resulting into a $(2s^1, 2p_x^1, 2p_y^1, 2p_z^1)$. configuration as visualized in Figure 2.2. These electronic orbitals do not bond separately but hybridize, i.e. mix in linear combinations, to produce a set of orbitals oriented towards the corners of a regular tetrahedron. The hybrid orbitals consisting of one s orbital and three p orbitals are known as sp^3 hybrid orbitals. The sp^3 hybrids allow a strong degree of overlap in bond formation with another atom and this produces high bond strength and stability in the molecules. The arrangement of bonds resulting from overlap with sp3 hybrid orbitals on adjacent atoms gives rise to the tetrahedral structure that is found in the lattice of diamond and in molecules such as ethane, C_2H_6. In these structures all the available electrons are tied up in strong covalent bonds, named σ-bonds. Carbon compounds containing σ-bonds formed from sp^3 hybrid orbitals are termed saturated molecules. The saturated hydrocarbons, in general, have high band gaps and, hence, are classified as insulators. Since conjugated

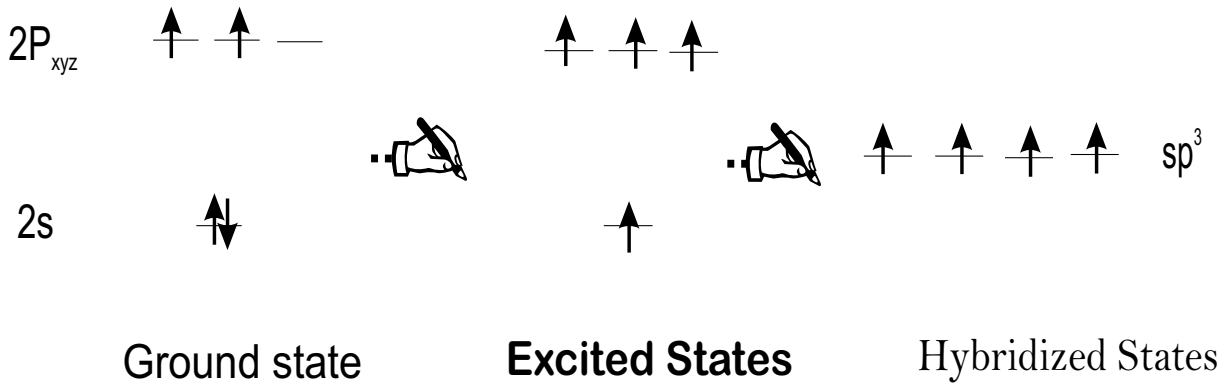

Figure 2.2: The outer shell electronic configuration of sp^3 hybridized orbital of carbon atom.

polymers composed of alternating single and double bonds, sp^3 hybridized orbitals cannot account for their electronic structure. Instead, the alternating single and double bonds are formed from sp^2 hybrid orbitals. Mixing of one s orbital with two of the p orbitals of C-atom forms 3 sp^2 hybrid orbitals, leaving one p orbital unhybridized (See Figure 2.3). The sp^2 carbon hybrid orbitals are known to form a different bond length, strength and geometry when compared to those of the sp^3 hybridized molecular orbitals. The sp^2 hybridization has one unpaired electron (π-electron) per C-atom. The three sp^2 hybrid orbitals of a C-atom arrange themselves in three-dimensional space to attain stable configuration. The geometry that achieves this is trigonal planar geometry, where the bond angle between the sp^2 hybrid orbitals is 120^o. The unmixed pure p_z orbital lies perpendicular to the plane of the three sp^2 hybrid orbitals(See Figure 2.4). The sp^2 orbitals give σ-bonds while the p_z orbitals form a different type of bonds known as π-bonds. The p_z orbitals of a polymer exhibit π-overlap, which results into a delocalization of an electron along the polymer chain. The π-bonds are, thus, considered as the basic source of conduction band in the conjugated systems. Polyacetylene is often considered as a model conjugated polymer. It has a simple, linear structure and exhibits a degenerate ground state. Figure 2.4 illustrates the arrangement of the σ -bonds and π-bonds in polyacetylene. Owing to its structural and electronic simplicity, polyacetylene is well suited to semi-empirical calculations and has therefore played a critical role in the elucidation of the theoretical aspects of conducting polymers.

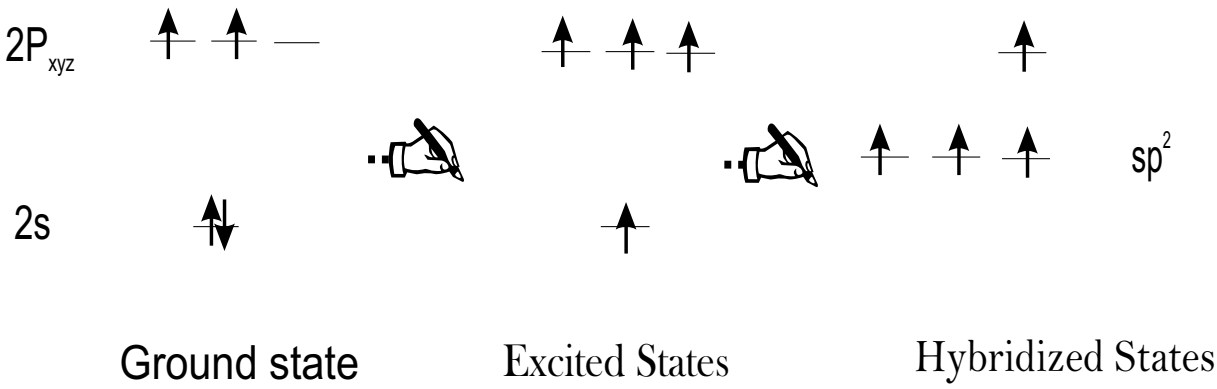

Figure 2.3: The outer shell electronic configuration of sp^2 hybridized orbital of carbon atom

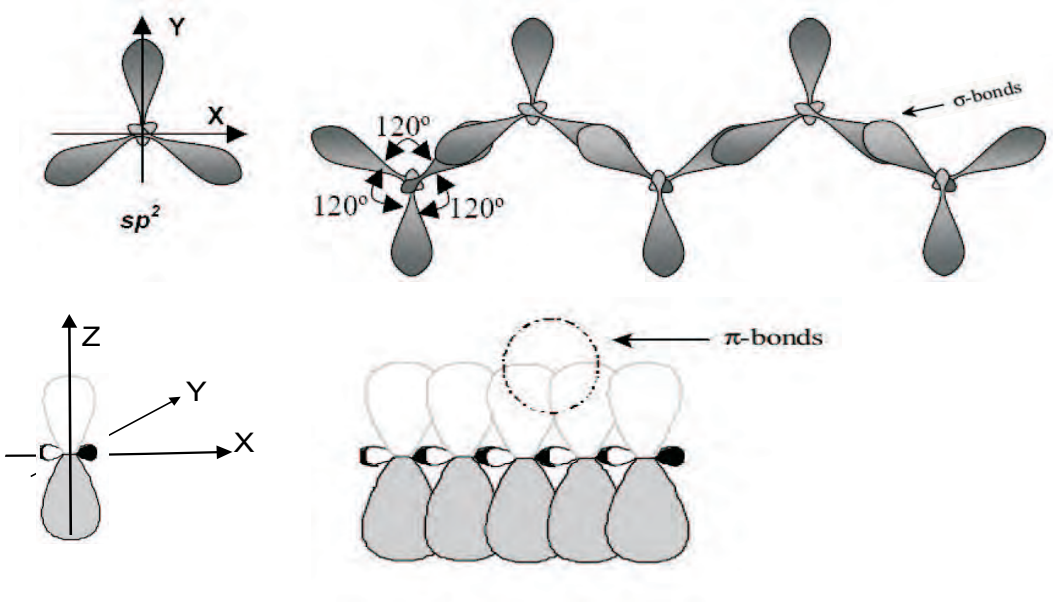

Figure 2.4: The configurations of conjugated polymers π-bones (above) and σ -bond (below) construction in conjugated polymers. (3) The chemical structure of a conjugated polymer poly(acetylene).

In terms of an energy-band description, the σ-bonds form completely filled bands, while π-bonds would correspond to a half-filled energy band (Figure 2.5). The molecular orbitals of a polymer form a continuous energy band that lies within a certain energy range. The anti-bonding orbitals located higher in energy (π^*) form a conduction band whereas the lower energy lying bonding orbitals form the valance band. The intermolecular interactions in the conjugated polymer chain are weak, the intermolecular distances are large, and the energy bands of the crystal are narrow. The two bands are separated by a material specific energy gap known as a band gap (E_g) (See Figure 2.5). The two separate bands are characterized by two quite important energy levels, namely electron affinity and ionization potential. The electron affinity of a semiconducting polymer corresponds to the lowest state of the conduction band (π^* state) or the lowest unoccupied molecular orbital (LUMO). Likewise, the ionization potential refers to the upper state of the valence band (πstate) and corresponds to the highest occupied molecular orbital (HOMO). The band gap of conjugated polymers determined from optical, electrochemical and other spectroscopic measurements is

within the semiconductor range of 1 to 4 eV, which covers the whole energy range from infrared to ultraviolet region of the electromagnetic wave .

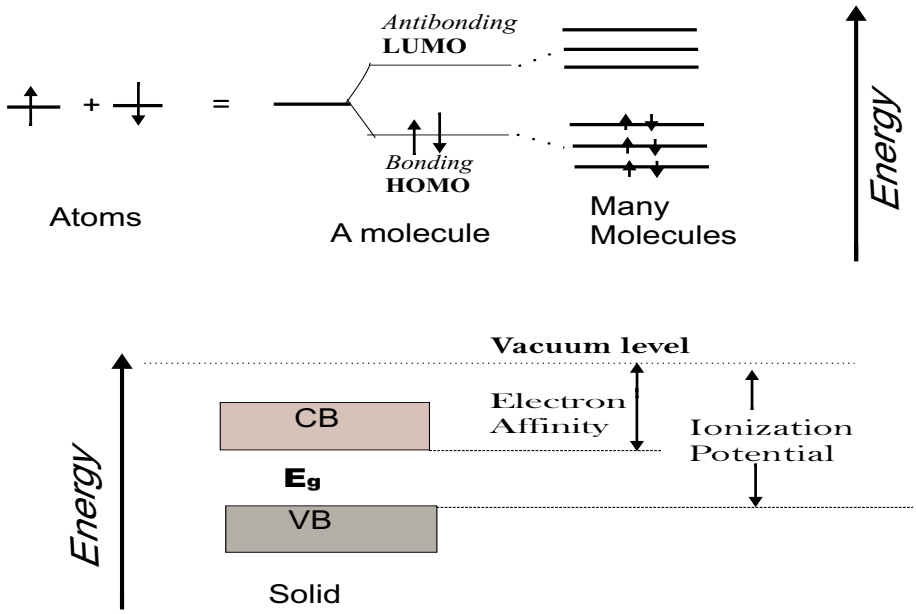

Figure 2.5: band formation in conjugated polymers from the molecular orbital theory.

2.3 Electrical conductivity of conjugated polymers

Conjugated polymers, in pristine and neutral states, are insulators with wide band gap or semiconductors with narrow band gap. However, this properties can be drastically changed by addition or subtraction of electrons to or from the conjugated chain with simultaneous intercalation of the compensating counter ions between the chains, a process called doping. There are several ways of doping conjugated polymers. For instance, charge injection and photodoping are the basic mechanisms that we use in our laboratory.

The insulating state may be realized by 1) simply filling a band with electrons (band insulator) or 2) the localization of electrons due to random potential (Anderson insulator) or 3) the localization of electrons due to the strong mutual repulsion of electrons (Mott insulator). If the Mott insulator is composed of multi-component particles such

as spin-up and spin down electrons or multi-channel electrons, it is categorized into three cases separated by the lower critical dimension of the component order. Namely, ordered insulator, disordered insulator and the valence band insulator. The metallic state of multi-component systems adjacent to the Mott Insulator is also classified into three types. ordered metal, disordered metal and band gap metals.

One way of looking at the nature of band gap in conducting polymers also stems from the periodic arrangement of the monomer units which can be regarded as one dimensional system. One dimensional approach theoretical calculations for the motion of electrons in metals produced important information such as band gap and other properties of metals. By treating electrons to be subject to periodic potential instead free charged particle in 1-D lattice; calculations were able to predict the existence of band gap in metals. Analogously, efforts were also made to understand the origin of the band gap in conjugated polymer by considering them as one dimensional system and using the concept of Peirls distortion theorem. Peirls theorem states that *a one dimensional monatomic metallic lattice with equidistant separation 'a' would be energetically unstable against a periodic lattice distortion*[1].

In the simplest conjugated polymer Polyacetylene (Figure 2.6), considering it as an extended chain with bond angle 180^o instead of 120^o, and then the main chain can be considered as one dimensional lattice. Thus, the alternating double and single bonds along the chain correspond to the short and long bond lengths, respectively. The double bonds are slightly shorter than the single bonds. Such arrangement of the bonds distorts the regular array of the lattice and doubles the elementary cell in real space corresponds to reducing the Brillouin zone by half in a reciprocal space. This introduces a discontinuity in the dispersion relation.

2.4 Elementary Excitations

From the theory of condensed matter it can be assumed that there exist a stable ground state and excited states of higher energy. In general, the energy of an excited state with respect to the ground state can be expressed as the sum of energies of elementary excitations or quasi-particles. This quasi-particles are the building blocks of the crystal in terms of motion. In organic materials, due to the dimerisation of the

bonds, they exhibit neither pure covalent nor pure polar bonds. They represent a separate class with regard to their bond nature exhibiting huge electron-lattice coupling compared to the inorganic solids. The strong electron-lattice coupling is responsible for the existence of the quasi-particles such as solitons, polarons and bipolarons in conjugated systems. These quasi particles can be identified by the additional energy levels associated with them which appear within the semiconductor bandgap see Figure.2.7 and 2.9. This can be observed using sensitive detection methods like photo-induced absorption spectroscopy[2,3].

Due to these reasons the photo-physics in this class of materials is often different compared to the inorganic semiconductors and not yet fully understood. One of the main differences is that photo-excitation in these materials does not automatically lead to the generation of free charge carriers, but to bound electron-hole pairs (excitons) with a binding energy of about 0.4eV while in inorganic semiconductors it is 0.16meV[2].

The quasi-particles that are created in conjugated polymers are:

- **Solitons:**-

  In polymers with degenerate ground states such as trans-polyacetylene there will happen a misfit (domain wall) when the degenerate states are in the same chain, see Figure 2.6. This defect site contains unpaired electron, the $2p_z$ atomic orbital of the C-atom at that site. At the Soliton site the atomic orbital is neither bonding nor anti-bonding rather it forms non-bonding state with energy in the middle of the band gap.

  This new energy state can accommodate up to two electrons. If one electron alone occupies this level, then the Soliton is neutral and carries a spin. The other two possible states are charged states with two electrons but without any net spin (s=0). Generally, soliton formation results in the creation of new localized electronic state that appears in the middle of the energy gap. For a larger number of solitonic state, the charged solitons interact with each other to form a soliton band, which eventually merge with the band edges to create true metallic conductivity[1,4]. New optical transitions associated with Solitons are observed in absorption spectra.

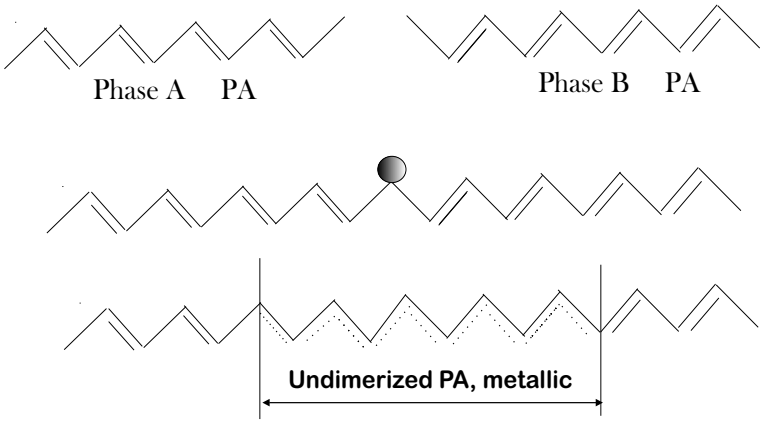

Figure 2.6: The formation of solitonic state in polyacetylene and the transition from insulating to conducting state.

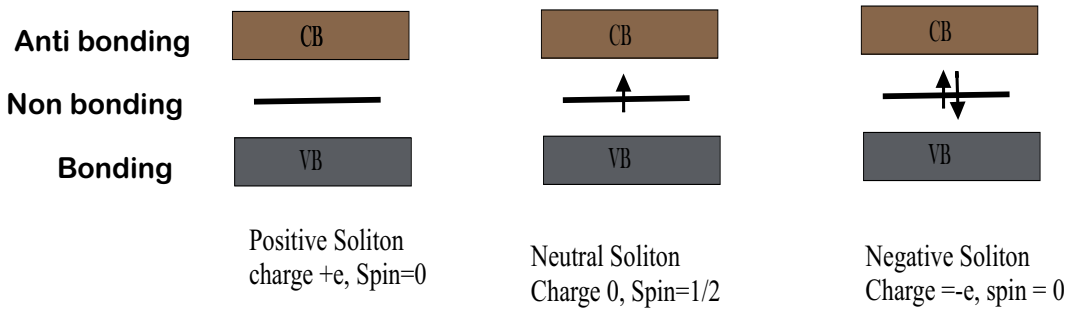

Figure 2.7: Formation of a mid-gap state. The anti-bonding (π^*) and the bonding (π) disappear into the conduction band (CB) and valence band (VB), respectively.

- **Polarons and Bipolarons:**-

The origin of the term polaron for charged quasi particles can be found in classical polar crystals where the associated charge e.g. the electron repulses adjacent electrons while attracting the nuclei resulting in a polarisation of the lattice in its closer vicinity. The formation of a polaron is regarded as a creation of two solitons in a single chain. These two defects are pushed by the lattice force and migrate to each other, minimizing the energy. This do not affect merely the polarisation in their vicinity they even change the nature of bonds from σ to π and vice versa via excitation and while traveling. This usually leads to a more rigid

structure in the excited state the so called quinoid configuration. Polyacetylene has a degenerate ground state. However, many other conjugated polymers have non degenerate ground state. For instance, in thiophene, the ring in the neutral and in the polaronic state as depicted in Figure 2.8, have different energies (The aromatic and Quinoidal configuration). In the polaron formation one of the

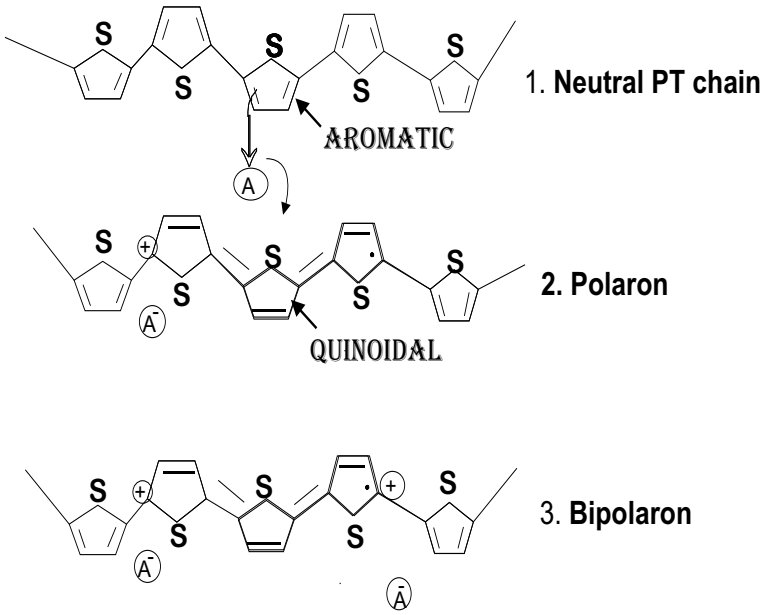

Figure 2.8: When the electron from a neutral PT is accepted by a doped accepter molecule, a PT polaron(a hole polaron) is formed. When two polarons bind they form bipolaron. It can also be viewed that the energy of the aromatic configuration (the ground state of PT) is less than the quinoidal (excited) state energy

solitons must be a neutral solution, and if the other is a positive soliton, then they form a (hole) polaron. In the event that both solitons are positive, they form a quasiparticle known as a bipolaron. Bipolarons are usually said to be formed when two polarons meet. The energy of two polarons is greater than that of a bipolaron. Hence, two polarons attract each other to form bipolarons while two bipolarons repel each other, whereas one polaron and one bipolaron can coexist freely passing each other. The two kinks in a polaron (and a bipolaron) give rise to two interacting states which are energetically separated states in the gap. Unlike the single mid gap state of a soliton. The schematics of the energy band

diagram for both polaron and bipolaron are depicted in Figure 2.8.

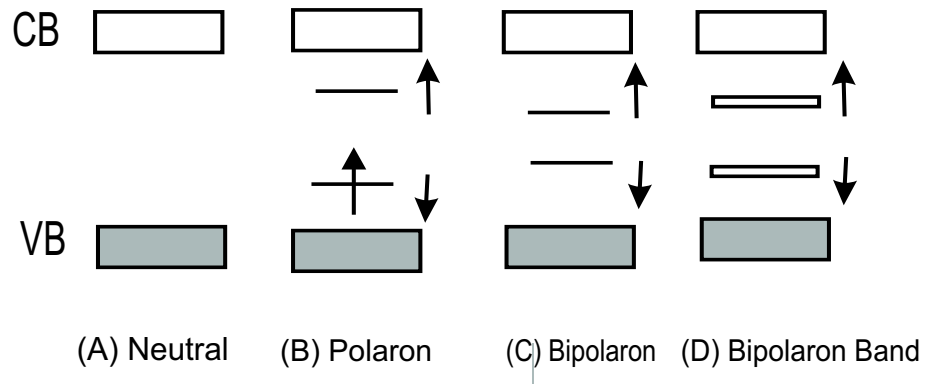

Figure 2.9: Polaronic and bipolaronic band gap formation in organic crystals.

2.5 Solubility of Conjugated polymers

In most cases, the preparation of thin film using spinning process require solution or melting the polymer. For experimental purpose, it is better to use a polymer solution to make thin films. Dissolving a polymer is a slow process that occurs in two stages. First, solvent molecules slowly diffuse into the polymer to produce a swollen gel. This may be all that happens, if for example, the polymer-polymer intermolecular forces are high because of cross linking, crystallinity, or strong hydrogen bonding. But if these forces can be overcome by the introduction of strong polymer solvent interactions, the second stage of solution can take place. Here the gel gradually disintegrates into a true solution. Only this stage can be materially speeded by agitation.
In dilute solution, where the polymer chain is surrounded by small molecules, the polymer molecule is in continual motion because of its thermal energy, assuming many different conformations in rapid succession. As the polymer melt is cooled, or as this molecular motion so characteristic of polymers is restrained through the introduction of strong interchain forces, the nature of the polymer sample changes systematically in ways that are important in determining its physical properties. The size of the molecular coil is very much influenced by the polymer-solvent interaction forces. In a thermodynamically "good" solvent, where polymer-solvent contacts are

highly favored, the coils are relatively extended, in a ”poor” solvent they are relatively contracted.

2.6 Working Principle of Organic Solar Cell

The conversion of solar light into electric power requires the generation of both negative and positive charges as well as a driving force that can push these charges through an external electric circuit. In organic semiconductors, absorption of photons leads to the creation of bound electron hole pairs (excitons) rather than free charges. These excitons carrying energy but no net charge may diffuse to dissociation sites where their charges can be separated. The separated charges then need to travel to the respective device electrodes, holes to the anode and electrodes to the cathode to provide voltage and be available for injection into an external circuit. To achieve substantial photovoltaic effect in PSCs, excited charge pairs need to be dissociated into free charge carriers through the assistance of electric field, bulk trap sites or interface of materials with different electron affinities.
In a first order simplified illustration that does not include other relaxed states such as polaronic states, we can comment the individual conversion steps with regard to the special situation in organic solar cells:

- **Absorption of photons**:- In most organic devices only a small portion of the incident light is absorbed. The very reason for this is first usually CPs have higher band gap say relative to Si (1.1eV). The other reason is the thickness of the active organic layer, they have typically low charge carrier and exciton mobilities, which requires layer thickness in the order of 100nm. This forces us to prepare a thin film, where only few of the photons will be absorbed.

- **Exciton diffusion**:- Ideally, all photoexcited excitons should reach a dissociation site. Since such a site may be at the other end of the semiconductor, their diffusion length should be at least equal to the required layer thickness (for sufficient absorption), otherwise they recombine and photons were wasted. Exciton diffusion ranges in polymers and pigments are typically around 10nm [4].

- **Charge separation**:- Charge separation is known to occur at organic semiconductor/metal interfaces, impurities (e.g. oxygen) or between materials with sufficiently different electron affinities (EA) and ionisation potentials (IP). In the latter one material can then act as electron acceptor (A) while the other keeps the positive charge and is referred to as electron donor (D) - since it did actually donate the electron to A. If the difference in IP and EA is not sufficient, the exciton may just hop onto the material with the lower bandgap without splitting up its charges. Eventually, it will recombine without contributing charges to the photocurrent.

- **Charge transport**:- The transport of charges is affected by recombination during the journey to the electrodes particularly if the same material serves as transport medium for both electrons and holes. Also, interaction with atoms or other charges may slow down the travel speed and thereby limit the current.

- **Charge collection**:- In order to enter an electrode material with a relatively low workfunction (e.g. Al) the charges often have to overcome the potential barrier of a thin oxide layer. In addition, the metal may have formed a blocking contact with the semiconductor so that they can not immediately reach the metal.

Chapter 3

Electrical and Photovoltaic Properties Of Organic Solar Cells

By definition, a photovoltaic effect is the development of voltage across an electrostatic potential barrier under the influence of light. In the classical photovoltaic effect, the electrostatic potential gradient exists in the dark and results from the presence of an interfacial region where the net majority carrier density has been reduced (depleted) from the bulk equilibrium carrier value. The depleted region is also called the space-charge layer.
The existing potential gradient assists in the generation, separation and migration of the charged carrier species produced by light. It is this "built-in" field that distinguishes photovoltaism from photoconductivity, where externally applied fields are required to produce current. Normally, in the absence of such an applied field, photo-generated species in a photoconductor simply recombine, giving no net current flow. Thus, a photovoltaic material must be photoconductive. A simple four-step description of the photovoltaic process might then be as follows.

- Photo generation of charged or neutral species.
- Charge separation or generation from neutral carrier species,
- charge transport, and
- charge collection to yield current.

In this chapter we will briefly discuss the photovoltaic property of an organic semiconductor material sandwiched in between asymmetric work function electrodes (Single layer PVDs structure). They are often referred to as Schottky type devices or Schottky diodes since charge separation occurs at the rectifying (Schottky) junction with one electrode. The other electrode interface is supposed to be of ohmic nature.

3.1 Metal-Semiconductor Contact

When a metal is in contact with a semiconductor, say n-type semiconductor, since in most cases rectifying contact is made with n-type semiconductor, there is diffusion of charge carriers from either side. The dark diffusion process depends on the relative vacuum level energy (E_{vac}) values of the materials, the work functions for the metal (ϕ_m) and the semiconductor (ϕ_{ns}) (n-type) [5]. Work function is the energy needed to take an electron from the Fermi-level (E_F) to the vacuum level (E_{vac}) where it is completely free.

When $\phi_m > \phi_{ns}$, electrons diffuse into the metal in order for the electrochemical potential of the electrons; or Fermi-level of both the electrode and the semiconductor to become constant through the system in thermal equilibrium (see Figure 3.1). Positively charged donor atoms remain in the semiconductor creating a space charge region. This is depicted by bending of the band near the interface. In the bulk of the semiconductor the relative level of E_F to E_v and E_c remains unchanged. In Figure 3.1b, the parameter ϕ_{Bn} is the barrier height of the semiconductor contact, the potential barrier seen by electrons in the metal trying to move into the semiconductor. This barrier is known as the Schottky barrier and is given ideally by:

$$\phi_{Bn} = \phi_m - \chi \tag{3.1}$$

where χ is electron affinity of the semiconductor. On the semiconductor side, V_{bi} is the built-in potential barrier. This barrier is the barrier seen by electrons in the conduction band trying to move in to the metal. The built-in potential is given by:

$$V_{bi} = \phi_{bn} - \phi_n \tag{3.2}$$

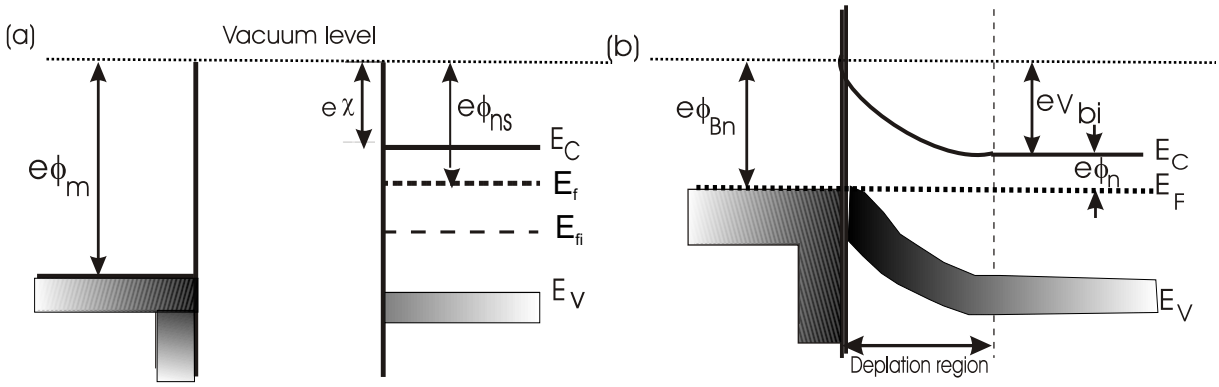

Figure 3.1: Energy band diagram of metal-semiconductor contact (a) before contact (b) after contact for $\phi_m > \phi_{ns}$. Where E_{Fi} is the intrinsic Fermi-level, $e\chi$ is electron affinity and $e\phi_n$ is the excitation energy of the semiconductor.

When $\phi_m < \phi_{ns}$, electrons diffuse into the semiconductor to achieve thermal equilibrium in the junction. This makes the surface of the semiconductor more n-type and the excess electrons exist essentially as a surface charge density. In this case, since there is no region which is depleted of majority carriers, such junctions form ohmic contacts, see Figure 3.2. By a similar analysis of metal-p-type semiconductor contact, we have the following general rules :

$$\begin{array}{lll} \phi_{ps} > \phi_m \quad or \quad \phi_{ns} < \phi_m & & \text{Schotky barrieres,} \\ \phi_{ps} < \phi_m \quad or \quad \phi_{ns} > \phi_m & & \text{Ohmic contacts.} \end{array}$$

If we apply a positive voltage (injection potential) to the semiconductor with respect to the metal for the case ($\phi_m > \phi_{ns}$), the n-semiconductor-to-metal barrier height increases, while ϕ_{Bn} remains constant. This bias condition is the reverse bias. On the other hand, if a positive voltage is applied to the metal with respect to the semiconductor, the semiconductor-to-metal barrier is reduced while ϕ_{Bn} again remains essentially constant. In this situation, electrons can more easily flow from the semiconductor into the metal since the barrier has been reduced. This bias condition is the forward bias [4].

Another point to be considered is the ability of majority carriers in the metal to further diffuse into the semiconductor. We will define two injection potentials, one for electrons ϕ_{ie} and one for holes ϕ_{ih}:

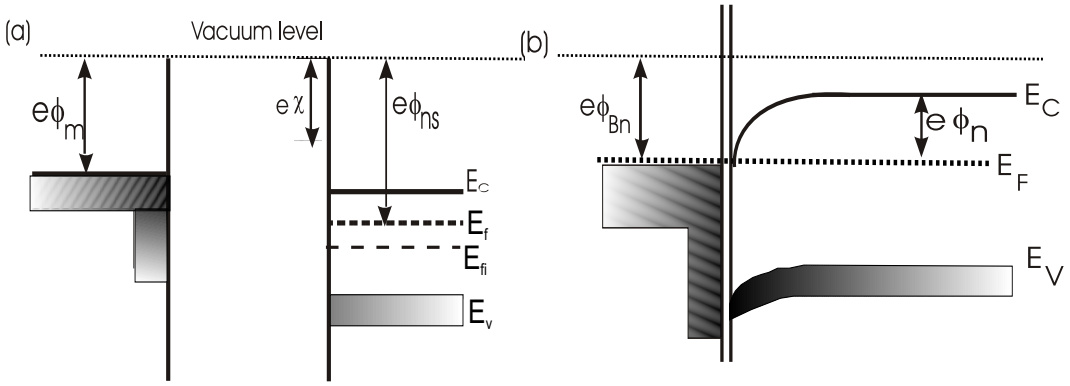

Figure 3.2: Ideal energy band diagram (a) before contact and (b) after contact for a metal-semiconductor (n) junction for $\phi_m > \phi_{ns}$.

$$\phi_{ie} = (\phi_m - E_c) + |e|V_{bi}$$

$$\phi_{ih} = (E_v - \phi_m) - |e|V_{bi}$$

we considered the metal as an infinite source and sink for carriers [1,6]. It can thus be seen that, if $|e|V_{bi} \leq (\phi_m - E_c)$ or $(E_v - \phi_m)$, the electrodes can be ohmic or injecting; they inject electrons if $\phi_m \approx E_c$ and holes if $E_v \approx \phi_m$. For $|e|V_{bi} > (\phi_m - E_c) or (E_v - \phi_m)$ no injection occurs. These electrode injection effects can contribute significantly to the observed photo currents [2,5,7] and also to our latter discussions on space-charge-limited currents [1,5,8]. ***Remember that the band pictures described so far do not account for any localized deviations in energy levels due to defects or surface states. Also remember that these electrostatic potentials exist in the dark***.

3.2 Dark I-V Rectifying Behavior and applied Voltages

If the electrostatic potential of the ohmic side of the semiconductor is raised by V relative to the blocking contact side, by means of an applied voltage (V_{app}) we no longer have the previous equilibrium situation. There evolves a new equilibrium potential

barrier $|e|V_{bi}$ due to further diffusion majority carriers.

$$|e|V = e(V_{bi} - V_{app})$$

Charge transport across the metal-semiconductor interface can arise from the following three process:

1. Transport of carriers from the semiconductor over the potential barrier into the metal. This is the dominant process for moderately doped semiconductors.
2. Field emission of carriers through the barrier.
3. Recombination in the semiconductor, this corresponds to minority carrier injection.

Neglecting the other mechanisms and considering the dominant thermionic emission related current, the current density-voltage characteristics of the Schottky diode is given by

$$J = J_o \left[\exp(\frac{-qV}{nk_BT}) - 1 \right] \tag{3.3}$$

where J is the total current density, J_o is the value of the reverse saturation current density, q is the charge on the electron, V is the applied voltage, k_B is the Boltzmann's constant, T is the absolute temperature and n is the diode quality factor. For most organic and many inorganic materials, particularly at low applied voltages ($\leq$ 0.4), the diode quality factor (n) must be added to fit experimental data to theory. Its value ranges from 1 to 3 and is usually taken as 2 [2].
For metal/semiconductor contacts, an explicit relationship between the barrier height (ϕ_b) and J_o can be obtained from thermionic emission / diffusion theory [3,5]:

$$J_o = A^{**}T^2 \left[\exp(\frac{-q\phi_b}{kT}) \right] \tag{3.4}$$

The exponential term, $\exp(\frac{-qV}{kT})$, represents the Boltzmann factor relating the electron concentration at the semiconductor surface, n_s, to the effective density of states in the semiconductor conduction band (N_c). The modified Richardson constant, A^{**}, express the probability that once an electron reaches the metal/semiconductor interface, it will successfully cross the metallurgical barrier and be injected in to the metal phase.

It also takes in to account the effective density of states in the conduction band, the effective mass of the electron in the semiconductor, phonon scattering of the electrons between the top of the barrier and the metal surface and quantum mechanical reflection at the metal/semiconductor interface [2,4].
The Richardson constant for an electron in free space, A, has a value $120\frac{A}{cm^2k^2}$ but the modified Richardson constant A^{**} is lower than A [5]. A^{**} is typically between 10 and $100\frac{A}{cm^2k^2}$. For organic semiconductor Schottky diodes the modified Richardson constant is assumed to be that of a free electron, namely, A^{*}=$120\frac{A}{cm^2k^2}$ [3].
Depending on the value of J_o with respect to J, we can have three types of contacts.

Case-1 For $J_o \ll J$, the contact will effectively block current flow for the reverse bias voltage but display an exponentially increasing current when the bias is forward bias. Such types of rectifying contact are desirable for photovoltaic cells [1,5], photon detectors, field effect transistors, chemical sensors [1], and other semiconductor devices.

Case-2 For $J_o \gg J$, the junction will readily pass current for both signs of the applied voltage. From eqn.3.3 with $J_o \gg J$, the exponential can be expanded to yield :

$$V = (\frac{-nkT}{qJ_o})\,J \tag{3.5}$$

Such a linear, ohmic contacts are necessary to avoid resistive losses for almost all types of semiconductor structure [4]

Case-3 For $J_o \approx J$, the contact display neither ohmic nor rectifying but symmetric J-V characteristics.

Experimentally the value of J_o is determined by applying a forward bias to the metal-semiconductor contact, and evaluating the intercept of the semilog plot of the J-V data (the lnJ versus V plot). Equations 3.3 and 3.4 yield the value of the barrier height (ϕ_b) which can be verified by plotting $\ln(\frac{J_o}{T^2})$ versus $\frac{1}{T^2}$, which should produce a line with a slope of $(\frac{-q}{k})\phi_b$.

3.3 Illuminated Current-Voltage Characteristics

For metal/semiconductor Schottky diodes, the dark current is mainly due to the majority carriers. But when the diode is illuminated with photons having enough energy for the creation of an electron-hole pair (exciton) in the depletion region, the electric field at the junction is able to separate the photogenerated charges by preventing recombination. So, the resulting photocurrent is mainly due to the minority carriers. Now, suppose we have a metal/n-type polymer Schottky diode as shown in Figure 3.3a. There is an accumulation of holes at the semiconductor side of the interface in the dark. When light is illuminated, the concentration of holes in the semiconductor decreases due to recombination with photogenerated electrons. This results in the formation of new effective Fermi-level ($E_{f,eff}$) when equilibrium is attained as shown in Fig. 3.3b.

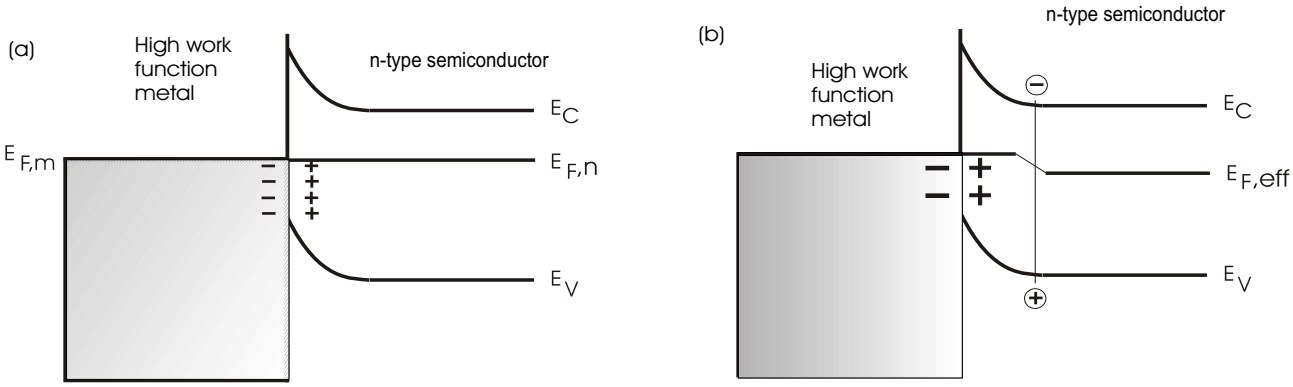

Figure 3.3: Energy band diagram of metal-semiconductor(n) (a)in the dark and (b) under illumination.

The total current under illumination is the sum of the photogenerated current and the thermally emitted current. Generally, the I-V characteristic of a photovoltaic device can be described by [2,3,5]:

$$I = I_o \left\{ \exp\left(\frac{e}{nkT}(V - IR_s)\right) - 1 \right\} + \frac{V - IR_s}{R_{sH}} - I_{pH} \tag{3.6}$$

where I_o is the dark current, e the elementary charge, n the diode ideality factor, V the applied voltage, R_s the series resistance, R_{sH} the shunt resistance, and I_{pH} is the

photocurrent. The corresponding equivalent circuit is depicted in Figure 3.4b. For highly efficient solar cells R_{sH} is very large to prevent leakage current and the series resistance is very low to get a sharp rise in the forward current. So for this case we have the following:

$$I = I_o \left\{ \exp\left(\frac{eV}{nkT}\right) - 1 \right\} - I_{pH} \tag{3.7}$$

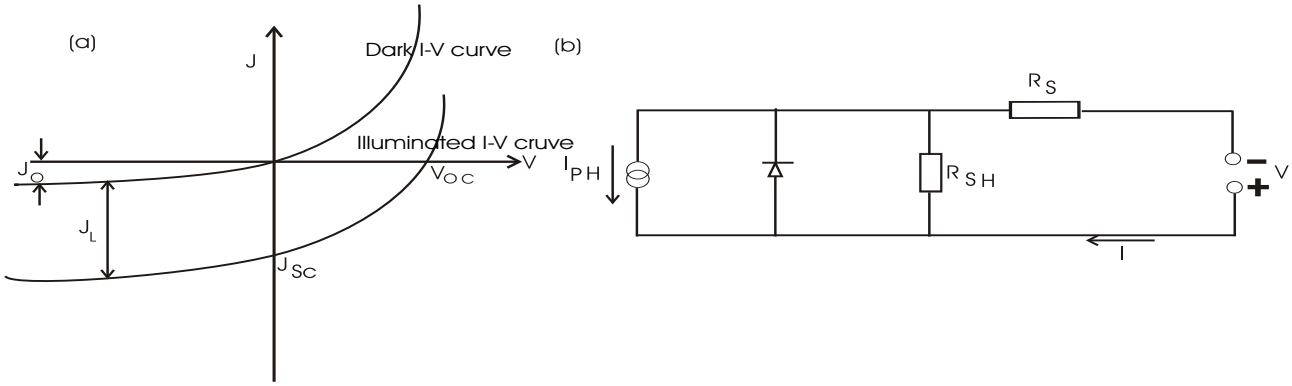

Figure 3.4: Figure (a) current-voltage characteristics of a photocell in the dark and under illumination (b) Equivalent circuit diagram for a solar cell, described by equation 3.6

3.4 Fill Factor and Power Conversion Efficiency

Fill factor (FF) and power conversion efficiency (η) are among the parameters that characterize a solar cell. Fill factor tells about the squareness of the fourth quadrant of the I-V curve under illumination. Mathematically, fill factor is defined as:

$$FF = \frac{I_{max}V_{max}}{I_{sc}V_{oc}} = \frac{P_{max}}{I_{sc}V_{oc}} \tag{3.8}$$

where I_{max} and V_{max} are values of corresponding current and voltage, respectively, when their product (power) is the maximum (P_{max}) of all corresponding products of current and voltage in the fourth quadrant of the I-V curve under illumination. I_{sc} and V_{oc} are short circuit current and open circuit voltages, respectively, see Figure 3.5. The values of V_{max} and I_{max} can be computed from the following equation

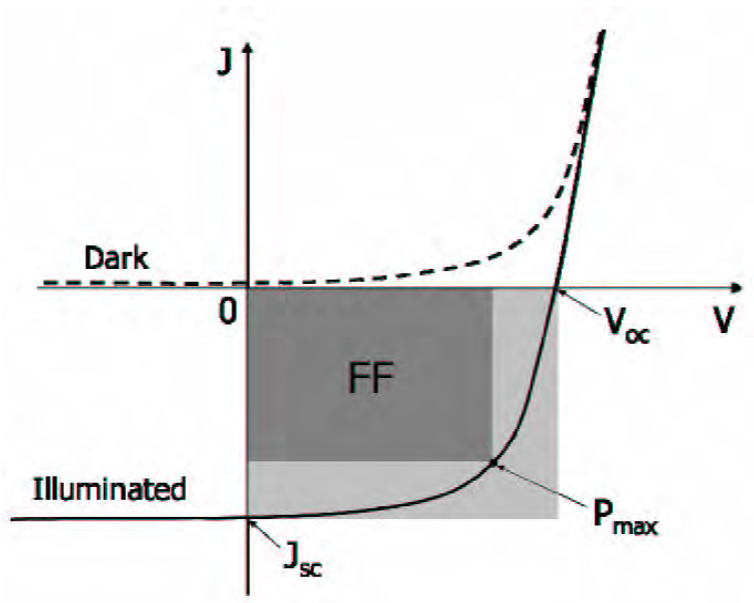

Figure 3.5: Typical I-V characteristics of an organic photo cell in the dark (dashed line) and illumination (solid line) conditions. The maximum out put power is given by the rectangle $I_{max} \times V_{max}$.

$$\frac{\partial P}{\partial V}\Big|_{V=V_{max}} = 0 \tag{3.9}$$

For an ideal solar cell FF=1. For inorganic solar cells, the fill factor is typically between 0.7 and 0.8 [8]. For undoped organic semiconductor solar cells, it assumes values less than 0.7[8,9]. The power conversion efficiency (η) of a solar cell is the ratio between the maximum output power (P_{max}) and the power of incident light (P_{in}).

$$\eta = \frac{P_{max}}{P_{in}} = \frac{I_{sc}V_{oc}FF}{P_{in}} \tag{3.10}$$

In general, the conversion efficiency of a solar cell in percentage is given by [3]

$$\eta\% = \left[\frac{I_m V_m}{P_{in}}\right] \times 100\% \tag{3.11}$$

or

$$\eta\% = FF\left[\frac{I_{sc} V_{oc}}{P_{in}}\right] \times 100\% \tag{3.12}$$

In general, to obtain the required efficiency from our solar cell, we have to get an optimized values of FF I_{sc} and V_{oc}. For organic solar cells based on polymer, the magnitude of I_{sc}, V_{oc} and FF depends on the parameters such as: light intensity, temperature, composition of the components, thickness of the active layer, the choice of the electrodes used, as well as the solid state morphology of the film [1,9]. In the next chapter we will dill how charge carriers are transported in the bulk of the polymer which has a great role in the development of solar cells with semiconducting polymer active films.

Chapter 4

Charge Carrier Transport in Organic Solids

Inorganic crystalline materials have well defined band transport properties due to the perfect overlap of their electronic wave functions. Free carriers, in such systems, are delocalized and have high mobility at room temperature. Also in crystalline organic solids such as Anthracene, in which the mobility is in the order of $1\frac{cm^2}{VS}$, the transport mechanism may be explained by a band theory formalism which posses a limit of $0.4\frac{cm^2}{VS}$. However, the solid-state phase of π-conjugated polymers is dominated by amorphous phases due to weak intermolecular interactions. The random distribution of conjugation length of polymer chains gives rise to distribution of electronic states, where regular lattice arrangement is lacking. Thus, a polymer film can be described as a discontinuously distributed amorphous phase, where the discontinuity is introduced by the small crystalline like ordered phases of small dimensions. The variation in molecular morphology leads to the broadening of the electronic density of states and results in hopping-type transport. The localized states put a lot of restriction on hopping transport thereby limiting the mobility of the charge carriers. Some organic systems, such as molecular crystals, form large-scale well-ordered phases that lead to substantial increase on charge carrier mobility. A brief description of hopping transport and experimental mobility measurement techniques in disordered materials, such as conjugated polymers, are discussed in this chapter.

4.1 Models of Hopping Transport.

Structural or chemical defects in the crystal introduce states in the forbidden energy gap, spatially localized at the defect sites. A mobile carrier from the transport bands may get trapped at such a defect state, and no longer contribute to the conductivity until it is released again. In addition to such delocalized band transport with multiple trapping, carriers may also tunnel directly from one localized state to another when the electronic wave functions of the defect states have sufficient overlap. The carrier may overcome the energy differences between the defect sites by absorbing the emitting phonons. This mechanism of phonon-assisted tunneling or "hopping", which was originally proposed by Conwell and Mott [7]. The transition rates for phonon-assisted tunneling were calculated by Miller and Abrahams [10,11]. Hopping from a localized state j to a state i takes place at a phonon frequency ν_o, corrected for tunneling probability and the probability to absorb a phonon for hops upward in energy:

$$W_{ij} = \nu_o exp(-2\xi R_{ij}) \begin{cases} exp(-\frac{\varepsilon_i - \varepsilon_j}{k_B T}), & \varepsilon_i > \varepsilon_j; \\ 1, & \varepsilon_i < \varepsilon_j \end{cases} \tag{4.1}$$

where, ξ is the inverse localization length, R_{ij} the distance between the localized states, and ε_i the energy at the site i. Since the hopping rates are strongly dependent on both the position and the energies of the localized states, hopping transport is extremely sensitive to structural as well as energetic disorder.
Hopping transport can also be well approximated by a random walk, which is restricted by energetic and spatial disorders. This typical disorder controlled transport is characterized by a considerable activation energy. Hopping transport mobility is, therefore, field and temperature dependent, where the mobility obeys the Poole-Frenkel law [10-14]

$$\mu = \mu_o exp(\gamma\sqrt{E}) \tag{4.2}$$

where μ_o is zero-field mobility, γ is field activation factor, and E is the net electric field. Disordered systems are subjected to an energetic spread of the charge transport sites, which are often approximated in shape by a Gaussian density of states (DOS). This shape is supported by the observation of Gaussian shaped absorption spectra of polymers [10]. The shape of the DOS is important for the description of the

charge transport as it reflects the disorder of the system. For disordered systems well approximated by Gaussian DOS, pioneering hopping transport model was proposed by H. Bässler [10,15]. This so called Gaussian disorder model (GDM) was developed through Monte Carlo simulation assuming a Gaussian distribution of transport site energy.

$$\rho(\varepsilon) = (2\pi\sigma_{DOS}^2)^{-\frac{1}{2}} exp(-\frac{\varepsilon^2}{2\sigma_{DOS}^2}) \tag{4.3}$$

where σ_{DOS} is the width of the Gaussian site energy distribution and the energy ε is measured relative to the center of the DOS. The Gaussian energy density of states is a direct manifestation of the energetic spread in the charge transporting sites of chain segments due to the fluctuation in conjugation lengths and structural disorder. Moreover, all the states within the Gaussian energy distribution are localized.

Mobility is a key parameter as far as transport issue is concerned. In particular, the efficiency of conjugated polymer based solar cells is substantially reduced due to their low charge carrier mobility. Hence, knowledge of mobility assists designing and identifying efficient polymers for solar cell and other applications. Consequently, mobility measurement in various systems is considered as a central subject of transport studies.

Usually in experiment mobility is measured using time of flight method and using field effect transistor. The other rather common method of measuring mobility in sandwich-structured devices is the space charge limited model (SCLM). The principle of this model is quite simple; charge injection into the bulk of a polymer film and I-V characteristics measurements are simultaneously performed. This technique does not describe transient phenomena since it is static in its nature. The SCLM is used to fit the SCL portion of the I-V curve thereby delivering mobility values. This method has successfully been used to investigate the field and temperature dependence of hole mobility in conjugated polymers [10,16-19]. This method can probe transport of charge carrier in solar cells and light emitting diodes that comprise thin films.

4.2 Formulation of Space Charge Limited Current.

Simulation of charge carrier transport in polymer-based devices is one of the major issues to be addressed in order to understand efficiency-limiting factors in PSCs. Despite the fact that in polymer films pure band transport is suppressed, the traditional charge transport laws, which were originally derived for inorganic materials, can still be applicable for organic materials as well. In this section formulation of SCLC model is described starting from basic transport equations.

PSC devices comprise thin (nano scaled) films of the active material. Consequently, charge transport in polymer-based diodes is often simplified as a one-dimensional process. In this context, the basic transport equations describing charge transport behavior are the one dimensional Poissons and continuity equations for electrons and holes. In particular, if the effects of traps are negligibly small, the drift-diffusion current equations and the Poissons equation, respectively, are given by

$$J_n = e[-\mu_n(x)n(x)\frac{d\psi}{dx} + D_n\frac{dn}{dx}] \tag{4.4}$$

$$J_p = e[-\mu_p(x)p(x)\frac{d\psi}{dx} + D_p\frac{dp}{dx}] \tag{4.5}$$

$$\frac{dE(x)}{dx} = \frac{e}{\varepsilon(p(x) - n(x))} \tag{4.6}$$

where $J_n(J_p)$ electron (hole) current density, n(x) (p(x)) is the electron (hole) density, $D_n(D_p)$ is electron (hole) diffusion constant, $\mu_e(\mu_p)$ is the electron (hole) mobility and ε = $\varepsilon_o\varepsilon_r$ with ε_o the permittivity of free space and ε_r the relative dielectric constant of the semiconductor. The electric field strength E(x) is related to the electrostatic potential $V(x)$ as $E(x) = -\frac{dV}{dx}$. The mobility and diffusion coefficients are related through the Einstein relation $D = \mu k_B T$, where k_B is Boltzmanns constant and T is temperature. Under the condition of SCL transport, the drift current dominates the net current flow and the diffusion part is often neglected.

Analytical expression of SCLC can be derived for a constant mobility and drift dominated transport. Under the assumption of an absence of traps, or negligible trap

density, solving the current equation together with the Poisson equation gives an analytical solution

$$J_{SCL} = \frac{9}{8}\varepsilon\mu\frac{V^2}{d^3} \tag{4.7}$$

where μ is the charge carrier mobility and d is the film thickness. Equation (4.7) describes a trap free SCL transport, often known as the trap free square law and Childs law for solids. When traps are present, most of the injected holes (electrons) are localized and do not contribute to current flow. In such cases, the dependence of current on voltage is determined by the density and energy distribution of the trap sites. Inclusion of single discrete traps into the analysis of the SCL current leads to $J \prec \frac{V^2}{d^3}$, while in the presence of traps with exponential trap distribution the SCLC takes a power law dependence of the form $J \prec V^{k+1}/d^{2k+1}$ [2] where k is defined in terms of a characteristics trap distribution constant.

4.3 Extraction of Transport Parameters from I-V Characteristics

The SCL method enables one to selectively study a single carrier transport in a solar cell. The freedom of having a single type of carrier in a device is adjusted by the choice of electrodes. In this section, practical examples of hole transport in solar cell materials using unipolar devices is presented and discussed.

Experimentally, it is possible to construct unipolar sandwich structured devices that give either electron dominated or hole dominated current flow. Both, the so-called electron only devices and hole only devices can be constructed by tuning charge injection barriers through appropriate choice of electrodes. Literally, the electrodes of electron only device should line up with the LUMO level of the semiconductor in order to discriminate hole Accumulation of charges in a bulk of a polymer film creates a field that reduces current flow. The net effect is the transition of constant mobility to field dependent mobility of the Poole-Frenkel type. Under this circumstance, the experimental SCL I-V characteristic is analyzed by solving the relevant current equations and Poissons equation together with the Poole-Frenkel mobility equation. Due to the field dependence of mobility, however, exact analytic solution cannot be

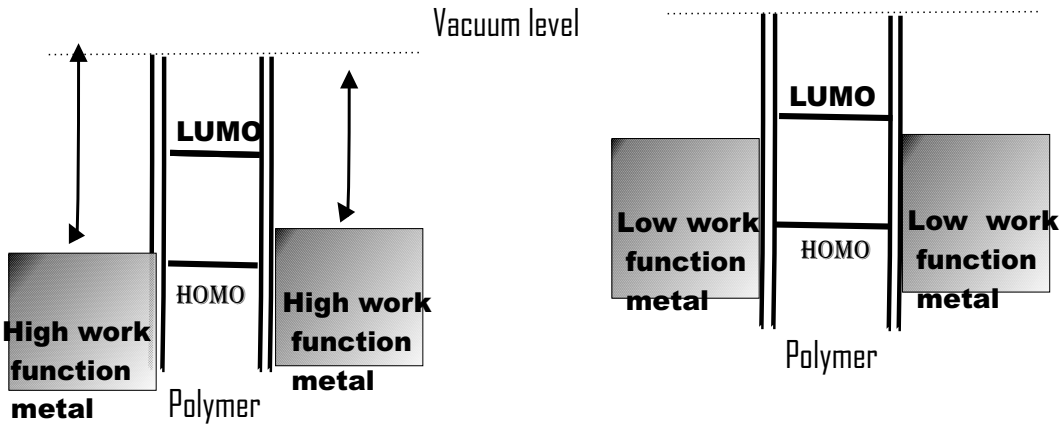

Figure 4.1: The geometry of hole only (left), and electron only (right) sandwich structured devices. The schematic diagram is shown for the case where the electrodes are not in contact with the polymer film.

obtained, which leads us to make numerical calculations. This method has been utilized to investigate hole transport [10,20] as well as electron transport [8,20] in thin polymer films sandwiched between coplanar electrodes. In this thesis, we have used the SCLM to investigate hole transport in PTOPT using the injection of hole from the Al electrode [12]. The energy levels of PTOPT and the work function of the electrodes are shown in Figure 4.2.

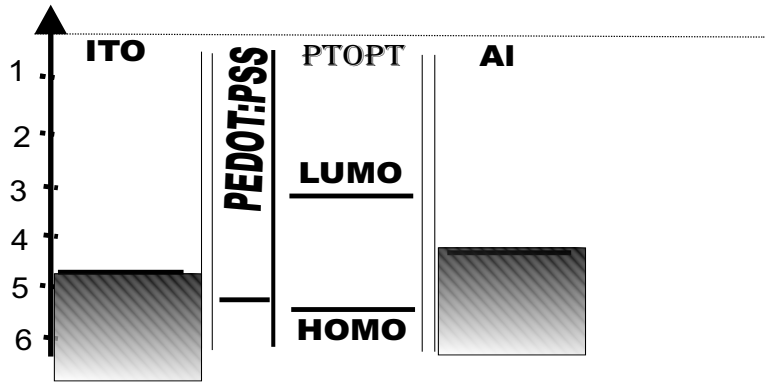

Figure 4.2: Energy level of the ITO/PEDOT:PSS/PTOPT/Al devices.

Chapter 5

Experiment

5.1 Sample Preparation

PTOPT is a low density polymer, which has a red color in its solid form. A photovoltaic device is constructed by sandwiching the polymer (PTOPT) film between glass/ITO/PEDOT:PSS and Al electrodes inorder to study its electrical properties and derive PV cell parameters. That is a metal- polymer-metal layer, **ITO/PEDOT:PSS/ PTOPT/Al** was formed. Briefly, the device is formed as follows: a commercially obtained ITO coated glass is prepared in a rectangular shape of dimension (*1.5cm x 2cm*). The thickness of the ITO is about 100 nm. Using a solution of concentrated hydrochloric acid, nitric acid and water with volume ratio of 48:4:48 respectively, we etch about one third of the ITO from the sample. The sample is then cleaned using a standard cleaning steps. After this the film layer will begin to be formed. First we spin cast a PEDOT:PSS solution on the glass/ITO sample using 3000rpm, which gives about 10nm thick film. Since the solution is formed using water as a solvent, the sample was baked for around 5 seconds to facilitate the evaporation of the solvent from the casted solution bubble. A solid PEDOT:PSS film will then be formed. Then the PEDOT:PSS which is coated on the pure glass side will be removed by a distilled water. After that PTOPT film were formed by spin coating from chloroform solution in a similar procedure, like the PEDOT:PSS. The concentration of the solution was $5gm/ml$. The thickness of the polymer that is formed at 1000rpm (which is about 120nm)[22]. After that some part of the polymer was removed from the two corners of

the ITO side (To get the ITO electrode for contact during measurement).
The last step in preparing the sample was to deposit the aluminium electrode by vapor deposition method. The Edwards vacuum depositor at 10^{-6} mbar was used to deposite the aluminium electrode on the polymer film. Finally, we get the sample which looks like Figure 5.1. The sample preparation was made at room temprature and 30% relative humidity level. The active area of all the diodes ware about $0.01cm^{-2}$.

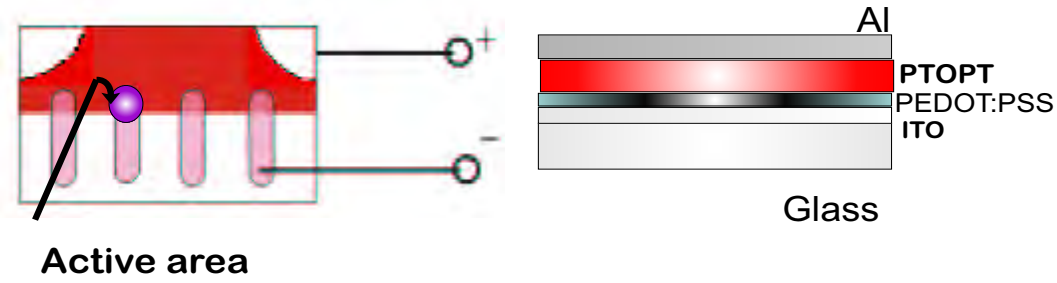

Figure 5.1: The first figure is a sample which contains a 4 parallel diode as is prepared in the laboratory. The second one is the cross sectional view of the metal-polymer-metal layer to one of the diodes.

5.2 Measurement Techniques

5.2.1 Absorption Measurement

For the absorbance measurement we prepare a polymer film on a transparent glass substrates. The absorption spectra were taken using PERKIN-ELMER UV / VIS / NIR Lambda-19 spectrometry. The spectra can also be used to calculate the band gap of the polymer based on the equation;

$$E_g = h\nu = \frac{hc}{\lambda}$$

where $h = 6.625x10^{-34} J.Sec$ is planck's constant, c is the speed of light and λ is the wavelength at which the absorption has started. This measurement also shows the wavelength at which a maximum absorption took place. We scan the sample for wavelengths from 300nm up to 900nm.

5.2.2 Current-Voltage measurement

To determine the I-V characteristics of the device produced, HP 4140 B PA meter DC voltage source and HP 16055 A-TEST FIXTURE interfaced with computer were used. During measurement, the sample was placed at room temperature. We apply a forward and a reverse bias voltage for the device under test (DUT). In the dark, scanning from -2.5V we take the reading of the current for every 0.05V step up to 2.5V by connecting ITO with the high terminal and Al with the low terminal of the dc source. Then by reversing the polarity the I-V data were taken by scanning from -4V up to 4V at same voltage interval. The latter measurement were intended to study the hole transport in PTOPT. For I-V measurement under a standard sun illumination, using a solar simulator Model $\#SS-50AA$ 1.5 Air Mass and $100mw/cm^2$ the forward bias voltage was scanned between $-1.2Vto+1.2V$ in steps of $0.05V$.

Chapter 6

Result and discussion

6.1 Absorption spectrum

The optical absorption of the polymer poly[3-(4-octylphenyl)-2,2'-bithiophene) (PTOPT) is given in figure 6.1. The figure indicates that absorption of electromagnetic radia-

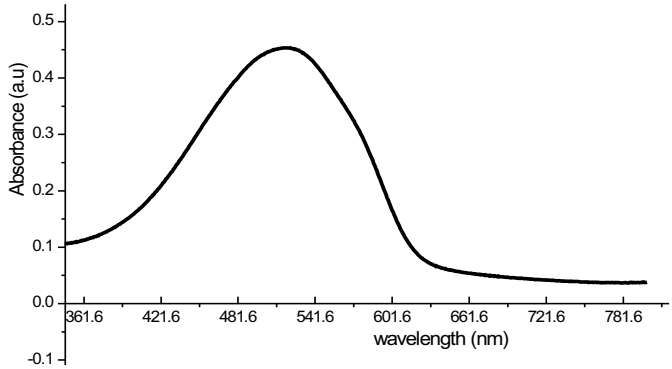

Figure 6.1: Absorption spectrum of PTOPT

tion took place in the visible range. The absorption started nearly at a wave length of 627nm. Using the relation $Eg = \frac{hc}{\lambda}$, the energy band gap, that is the minimum absorbed energy where there is at least an inter band transition of electrons, is determined to be 1.98eV. This tells us that the polymer is in a semiconductor category,

thus it can be used for manufacturing photovoltaic device.

6.2 J-V characteristics under dark

In order to understand the photovoltaic properties of the device, the J-V characteristics of the cell under dark region were studied. Employing the Al electrode connected to the negative terminal of a dc source and the PEDOT:PSS/ITO with the positive terminal we collected the current value for different voltage. The J-V curve of the Al/PTOPT/PEDOT:PSS/ITO sandwich structure in the dark is given in Figure 6.2. As

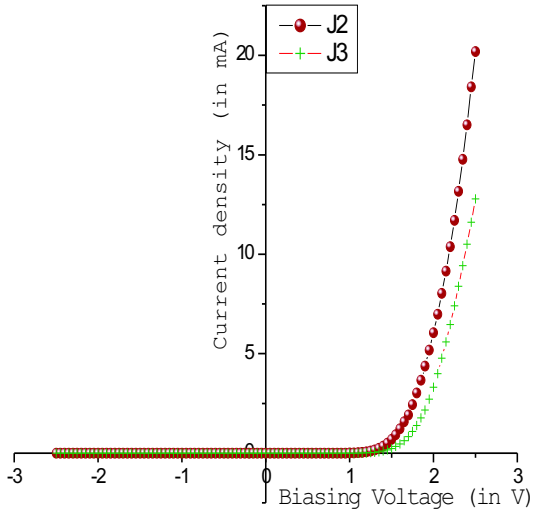

Figure 6.2: J-V characteristics under dark

it is seen in the figure, the J-V characteristic of the sample in the dark is non-ohmic and asymmetric. At low bias voltages ($V < 1.25V$), the current is almost blocked but for the higher forward bias voltages ($V > 1.25V$), the current increases exponentially. This is due to the injection of charge carriers from the electrodes. This fact confirms that a Schottky barrier rectifying contact is formed at the interface between Aluminium and the polymer. For the above J-V curve, the rectification ratio, $\frac{J_+}{J_-}$ at $\pm 2.5V$ was determined to be 10.25×10^3.

The semi-log plot of the dark I-V characteristic of a diode has several other features that correspond to various types of charge transport within the device, see figure 6.3. From the plot of $ln(J)$ versus V under forward bias conditions, three main features is revealed. The first one is the low bias regime (R1) which is characterized by an

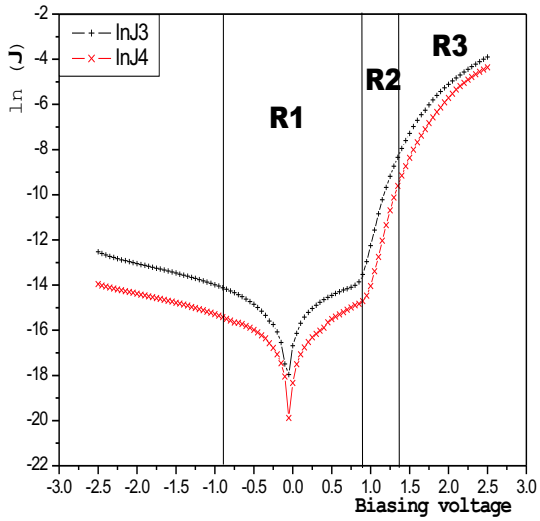

Figure 6.3: Semi logarithmic plot of the dark I-V characteristic

ohmic flow of charges which is formulated as $J \approx \frac{V}{d}$ where V is the applied bias voltage, J is the current density and d is the the thickness of the active semiconductor layer. Due to the low bias voltage, the injection of charge carriers from the electrodes to the semiconductor material is small. The second region (R2) is found for intermediate values of bias voltages. This region is characterized by a sharp slope which shows injection-limited current and the current increases exponentially with bias voltage. The injection limited conduction is commonly described by Richardson Schottky thermionic emission $J \prec exp(\frac{eV}{K_B T})$ [3]. The third regime (R3) corresponds to a high bias voltage values. It is characterized by flat band condition in which the built-in potential of the diode is compensated by the applied voltage. The effective barrier height is given by $V = V_{bi} \pm V_{app}$ (- for the reverse bias and + for forward bias). V_{bi} is the built-in potential under thermal equilibrium when the Aluminium makes

contact with the polymer. V_{app} is the applied voltage. So, at high forward bias voltage, the injection becomes enormous. The transport of charge flow is now dominantly controlled by the space charge limited current resulting in to saturation current.
From the second region (R2) of Figure 6.3, we can still discuss some properties of the sample. By extrapolating the straight line portion of this injection limited region (see Figure 6.4), the curve ln (J) Vs V for small positive voltage, usually very close to $V = 0V$, one can determine the value for the reverse saturation current. So, from

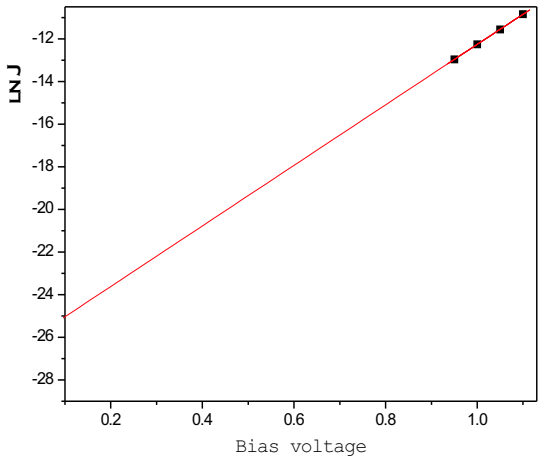

Figure 6.4: The extrapolated plot of the linear region of the J-V Semi logarithmic plot in the dark.

the graph, the reverse saturation current density is determined to be about $1.388 \times 10^{-11} mAcm^{-2}$. This J_o is small compared with the current density of the experimental interest($\sim 10^{-7} mAcm^{-2}$), where one can consider that the contact will effectively block current flow for the negative applied voltage. Once J_o is found, the barrier height per unit charge can be determined using the relation $\phi_b = \frac{kT}{q} ln(\frac{A^* T^2}{Jo})$. where, $\frac{K}{q} = 8.62 \times 10^{-5}$, $T = 298K$, $A^* = 120 \frac{A}{cm^2 K^2}$, the barrier height is found to be 1.08 eV. Another important parameter to be calculated is the diode ideality factor or quality factor n. From the slope of the graph, $(\frac{\triangle lnJ}{\triangle V})$, one can calculate the ideality factor using the relation $n = \frac{q}{KT} (\frac{\partial lnJ}{\partial V})^{-1}$. The diode ideality factor is calculated to be 2.94. For an ideal diode n=1 an increase in n tells us that there is an increase in the reverse bias

saturation current density (J_o). This informs us that the dark current-applied voltage curve showed rectification (the device behaves as a diode). The applied voltage can be used to alter the effective voltage across the device. When a reverse-bias voltage V_{rev} is applied to a contact region built in potential (V_{bi}), the effective barrier voltage V will be enhanced:

$$V = V_{bi} + V_{rev} = V_{bi} - (-V_{app})$$

If a forward-bias voltage V_{for} is applied, V may be smaller than V_{bi}, completely illuminated ($V_{for} = V_{bi}$), or even have a sign opposite that of V_{bi}; that is the contact becomes nonblocking, injecting, or ohmic.
It can also be seen that if $V \simeq nkT$, where T is now the ambient device temperature, majority carriers in the semiconductor have enough thermal energy to overcome the electrostatic potential barrier and carriers in the electrodes may also have enough energy to overcome the injection potentials [2,5]. Electron tunneling or field emission can occur through thin surface barriers, such as between electrodes and a material.

6.3 J-V characteristics under illumination

From the illuminated J-V data, an average fill factor of 0.2, open circuit voltage 990 mV, short circuit current density 16.23 Am^{-2} and power conversion efficiency of 0.328% were obtained. These are the basic parameters which determine the photovoltaic property of a device. In short, the devices shows an interesting photovoltaic property. Figure 6.5 shows the I-V curve for the two different diodes from our sample under illumination of AM1.5, one sun of intensity $100m\frac{W}{m^2}$. As one can clearly observe, when the V_{oc} increased the I_{sc} decreases and viceversa. The power conversion efficiency of a solar cell is affected by J_{sc}, V_{oc} and FF in addition to device structure and material properties. J_{sc} is affected by generation and dissociation rates of excited states as well as mobility of free charge carriers. The optical absorption of most polymers covers only the visible range of the solar spectrum. This leads to a decrement in the power conversion efficiency because, a substantial solar energy is located in the red and infrared region. This problem can be avoided if we have thick films, so as to absorb the red and the infra red ones, which have a large skin depth. But, making thick films increases the probability of recombination of charge carriers. The

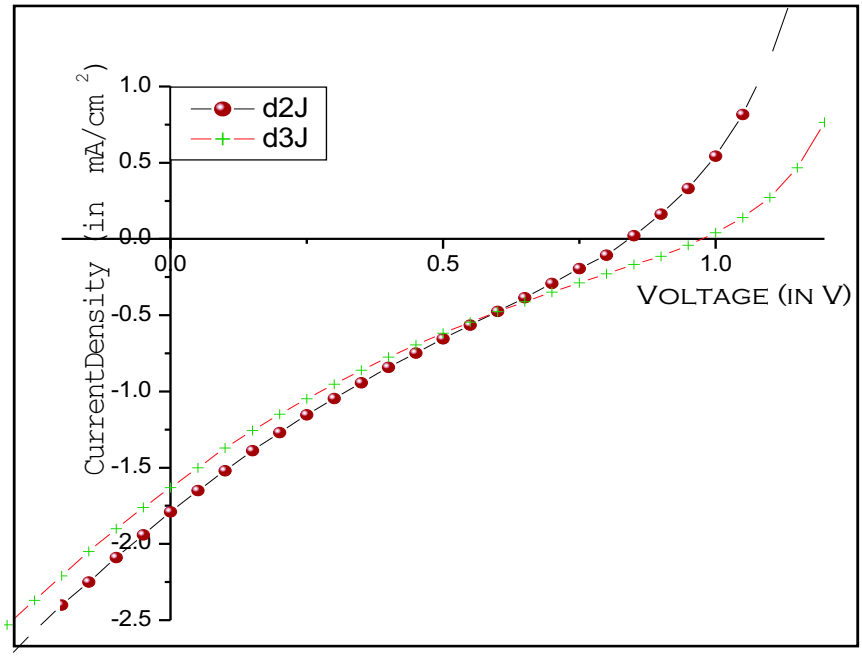

Figure 6.5: J-V curve under illumination

obtained FF is very low which can be attributed to poor transport property of the sample. Since they are the basic parameters in understanding the power conversion of our device it needs to be investigated how to get an optimized value of the I_{sc} V_{oc} and the FF of solar cell devices. From table 6.1, the FF of our diodes is 0.21, it is

Diode No	$I_{sc}(A/m^2)$	$V_{oc}(V)$	$P_{max}(W)$	FF	η in %
d_1	18.1	1.05	4.06	0.21	0.41
d_2	17.9	0.84	3.37	0.22	0.34
d_3	16.3	0.97	3.12	0.20	0.31

Table 6.1: Tabulated value of photovoltaic parameters of three different MSM contacts in a sample. The active layer of the sample was coated at 1000rpm.

relatively in the good FF range for organic solar cells but is a less value as compared to the commercially available inorganic (Si) solar cells. A FF of 0.6 is also reported in organic bulk-heterojunction solar cell, which is made from homogenous mixture of a polymer and electron accepter molecule [4]. Thus by using an electron accepter

molecule, which is in a good interaction of the electrochemical energy of PTOPT, we can maximize the current which is collected through our device. Also of great interest of physics is how charge carriers are generated and transported in the device. From the semi logarithm J-V plot which is measured under dark, by applying a forward bias voltage, we showed three different regions based on the nature to the current which is collected from the two electrodes. One of the objective of this thesis is to investigate the nature of charge carrier transport in the active layer of of our diode, specifically the hole transport from the dark J-V measurement which is by applying a reverse bias voltage. The value of the electrochemical energy level (HOMO and LUMO) of PTOPT and the work function of the electrodes (Al, and ITO) helps to assume that hole is injected into the polymer when the Al is connected from the high terminal of the dc potential difference source.

6.4 Hole transport in PTOPT

So far we have focused mainly on the diffused motion of the charge carriers across the device which were generated thermally and by photons. However, at high field direct emission of charge carriers from electrodes is particularly important. The process of charge-carrier injection under high fields at low temperatures has given rise to its own discipline, low temperature inelastic electron tunneling spectroscopy in which current fluctuations as a function of voltage are correlated with interfacial and bulk infrared group vibrational frequencies [5].

At higher temperatures, the influence of electrode processes on the apparent electrical properties has received much attention. It is assumed that, once the charge carrier is inside the solid, it does not know its origin. It recognizes only the influence of temperature, the local electric field (which may be affected by the way in which the charge carrier enters the solid), and the molecular nature of the material. This means that it is also possible to use controlled injection to study charge-carrier behavior within the solid. From cyclic voltammetry measurements, PTOPT has a HOMO level of 5.1eV and a LUMO level of 2.8eV [23]. The work function of Al is about 4.3eV, and that of PEDOT:PSS is about 5.2eV, the schematic representation of the device is shown in Figure 4.2. As can be inferred from the I-V characteristics, which is depicted

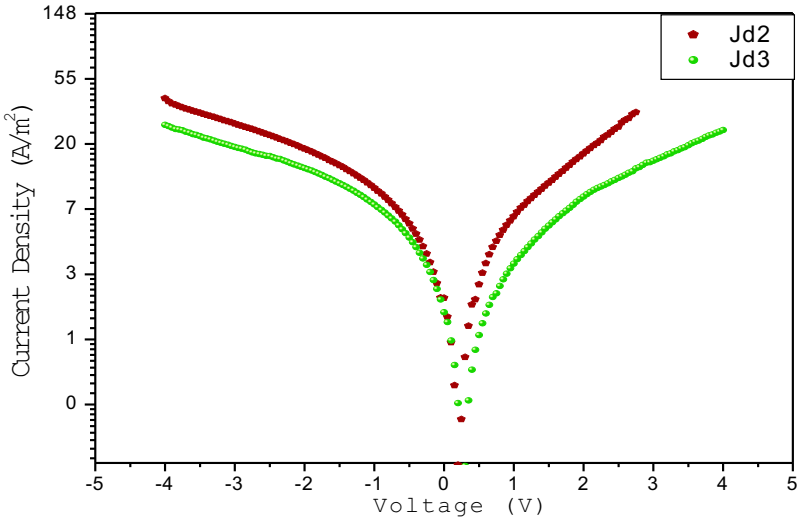

Figure 6.6: Semilog plot of the dark J V data which is measured by connecting the ITO with the low and Al with the high terminal of the dc source.

in Figure6.6, the non rectifying, and almost symmetric behavior is an indication of the existence of a relatively high barrier or a negligible built in potential. Consequently, it can be concluded that the current in the ITO/PEDOT:PSS/PTOPT/Al devices is limited by the hole injection into the HOMO of PTOPT through Al (+ on the Al) and electron injection into the LUMO through ITO/PEDOT:PSS (negative side). However, due to the high work function of PEDOT:PSS, electrons are not injected into the LUMO of the PTOPT. A similar result is reported in Al/P3HT contact [12], which has a similar electro chemical energy level when compared to the Al/PTOPT.

At low voltages the injected charge density is small so that the overall behavior is ohmic. As the voltage is increased, the number of injected carriers increases, so that space charge accumulates, tending to limit the current. This can be observed in Figure6.6. One can also observe that there is a linearity for higher voltages (in the space charge limited region) in the same figure. The linearity suggests that the injected charge overwhelms the transport capabilities of the polymer. This gives rise to the accumulation of positive charge near the Al hole injecting electrode. That is the bulk properties starts to control the current-voltage characteristics.

Using the space charge limited region of the reverse biased J-V characteristics under dark, the field dependance of the hole mobility across the electrodes was studied. The numerical fits to the experimental I-V curves are shown in Figure 6.7. The good agreement between the experimental and the calculated curves (from equations 4.2 and 4.7) enabled us to calculate the zero field hole mobility (μ_o) and field activation factor(γ) at room temperature. The thickness of the material (L) was estimated to be

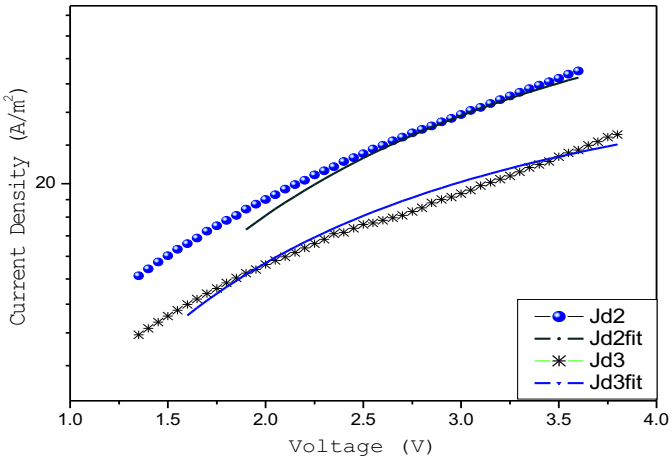

Figure 6.7: The fit of the space charge limited current region of the plot of the J-V curve under dark with the numerically calculated values.

120nm. The electric field (E) through the device is E = $\frac{V}{L}$. ϵ_r = 3, $\epsilon_o = 8.85 \times 10^{-12} \frac{c}{Vm}$, applying these values and the rearrangement of our equations gives us J(A/m^2) = 4.7 $\times 10^{11}$ μ $_o V^2$ $exp(\gamma \sqrt{\frac{V}{120nm}})$. From the fit of this equation with the curve the zero field mobility ($\mu_o = (2.25 \pm 0.12) \times 10^{-10} m^2/Vs$) and the field activation factor ($\gamma = (7.01 \pm 0.58) \times 10^{-5} (m/V)^{\frac{1}{2}}$).

These values are of the order of the the previously measured values of zero field mobility and the field activation factor of other polymers [10,12]. Therefore, these values can be used for further investigation of electrical and morphological properties of the polymer (PTOPT).

Conclusion

In this thesis, the photovoltaic and hole transport properties of ITO/PEDOT:PSS/PTOPT/Al was investigated. The polymer PTOPT shows good absorbance in the visible region of the electromagnetic spectrum where the absorption peak starts at a wave length of around 627nm, where it gave us that the band gap of PTOPT is 1.98eV. A Schottky diode is made with a quality factor (n = 2.94) rectification ratio of 1.03 $\times 10^4$. By connecting the ITO with the positive terminal of dc source and the aluminium (forward bias) with the low terminal, the photovoltaic property of the device was measured. The power conversion efficiency of the device was found to be around 0.35%. From the measurement which is made by reversing the polarity of the electrodes, it was observed that there was a hole injection from the Al to the active layer. As a consequence, so in the space charge regime of the J-V characteristic, the device will be hole injection. For higher fields, (for V $\geq$ 1.4V or E $\geq$ 1.17 $\times 10^7 \frac{V}{m}$) it was shown that the experimental data fit with the numerically obtained value.

Bibliography

[1] S.M.Sze *Physics of Semiconductor devices*, Second edition A Wiley-Interscience publication. New York.

[2] Martin Pope Charles E. Swenberg. *Electronic Process in Organic crystals* 1982 Oxford Universiy press.

[3] Bantikassegn Workalemahu, Linköping Studies in Science and Technoloty. Dissertations No. 144, Linköping 1996, Sweden.

[4] *Organic Solar Cell Architectures*, PhD Thesis by Dipl.Ing. Klaus Petritsch, Cambridge and Graz, July 2000.

[5] Donald A. Seanor *Electrical Properties of Polymers* 1982 Academic Press New York.

[6] D.A.Neamen, *Semiconductor Physics and Devices: Basic Principles*, 1992 New York.

[7] A. Fujimori, Springer Series in Solid-State Science *119 Spectroscopy of Mott Insulators and Correlated Materials*.

[8] P.M. Borsenberger, J.Appl. Phys. 68(10), 15 November 1990.

[9] Andrew C. Grimsdale, Philippe Leclere, Roberto Lazzaroni, J. Devin Mackenzie, Craig Murphy, Sepas Setayesh, Carlos Silva, Richard H. Friend, and Klaus Mullen. Adv. Funct. Mater. 2002, 12 , No. 10, October.

[10] A. Gadisa et al. organic electronics ORGELE 168 22 Feburary 2006.

[11] Allen Miller And Elihu Abrahams, Phys Review Vol 120, Number 3, November 1. 1960.

[12] Z. Chiguvare, J.Parisi, and V. Dyakonov. Journal of Appl. Phys. Vol. 94 Number 4, 15 August 2003.

[13] H.C.F Martens P.W.M.Blom, H.F.M. Schoo, Phys Review, B61 7489(2000).

[14] C. Tanase, P.W.M. Blom, and D.M.de Leeuw, Physical Review, B70 193202 (2004).

[15] H.Bässler Phys. Stat. Sol (b) 175. 15 (1993).

[16] Murray A. Lampert, Physical Review Volume 103, Number 6, september 15 1956.

[17] Michel Cornelis Josephs Marie Vissenbrg, Opto-Rlectronic properties of disorderd organic semiconductors. geboren teSint Maarten in 1972.

[18] S.Sinha and A..Monkman, Journal of Applied Physics, Volume 93, Number 9. 1 May 2003.

[19] Yu.N.gartstein^{l,a,b}, E.M. Conwell ^{a,b}, Chemical Physics Letters 2451(1995) 351-358.

[20] P.W.M. Blom, M.C.J.M. Visssenberg, A Review Journal Materials Science and Engineering, 27 (2000) 53-94.

[21] http//www:selfhealingmaterials/index-eng.htm, 1^{st} International conferance on self healing materials 18-20 April 2007, Noordwijk, The Neterlands.

[22] Fred W. B. Billmeryer, JR. *Textbook of polymer science* singapore New York. Chichester. Brisbane. Toronto.

[23] Tomas Johansson, Wendimagegn Mammo, Electrochemical bandgaps of substituted polythiophenes. Journl of Materials chemistry. 7^{th} April 2003.

DECLARATION

I the under signed declare that the thesis is my original work, has not been presented for a degree in any other university and that all sources of material used for the thesis have been duly acknowledged.

Bizuneh Gebremichael

Signature: _____

This Thesis has been submitted for examination with my approval as university advisor.

Dr. Genene Tessema

Signature: _____